Geochemical Perspectives Letters EAG

Water storage in the refractory lithospheric mantle

B.-X. Su, W.-F. Zhang, Q.-Q. Pan, Y. Bai, M.-M. Cui, X. Liu, I. Uysal, X.-P. Xia, X.-Y. Gu

Supplementary Information

The Supplementary Information includes:

- Methods
- Tables S-1 to S-4
- Figure S-1
- Supplementary Information References
- Additional References for Data Sources in Figures 2 and 3

Methods

Major element analysis

Major element compositions of olivine were measured using the JEOL JXA8100 electron probe microanalyzer at the Institute of Geology and Geophysics, Chinese Academy of Sciences. The operating accelerating voltage was 15 kV and beam current was 20 nA with a focused beam (spot diameter ~ 5 µm). The natural minerals and synthetic oxides that were used calibration are as following: albite (Na and Al), bustamite (Mn), diopside (Ca, Si, and Mg), K-feldspar (K), rutile (Ti), Fe_2O_3 (Fe), NiO (Ni) and Cr_2O_3 (Cr). Two TAP analytical crystals were used to analysis Na, Mg, Al, and Si (Kα), one LIFH crystal was used to analysis Cr, Mn, Fe, and Ni (Kα), and one PETJ crystal was used to analysis K, Ca, and Ti (Kα). Sodium and K were first measured in order to minimize the loss of volatiles by electron beam irradiation. The spectral line adopted of each element is Na (129.057), Mn (146.180), K (120.399), Mg (107.574), Si (76.815), Fe (134.638), Al (90.119), Ca (108.276), Ti (89.039), Cr (159.315), and Ni (115.218), respectively. The peak counting time for each element was 10-20 s. The detection limits are (1σ) 0.02 wt. % for Mg, Al, Si, Cr, K, Mn, Ti, Ni, and Fe, 0.03 wt. % for Na and Ca. A program based on the ZAF procedure was used for data correction. Detailed EPMA analytical conditions and results are shown in Table S-2.

SIMS analysis of water

Water contents in the olivine were measured using a CAMECA IMS 1280-HR secondary ion mass spectrometry (SIMS) at the State Key Laboratory of Isotope Geochemistry, Guangzhou Institute of Geochemistry, Chinese Academy of Sciences, following the method outlined by Zhang *et al.* (2020). Prior to analysis, samples were placed on doublesided adhesive tape and enclosed in a tin-based alloy. This alloy mount was then photographed under microscope (reflected light) and then gold-coated (~30 nm thick). This innovative sample preparation method enhances the vacuum condition within the sample chamber, yielding a smooth surface that improves detection limits and precision (Cui *et al.*, 2024).

When SIMS was maintained at the optimum condition after thorough baking, an automatic liquid nitrogen refilling system was used to maintain ultra-high vacuum in the sample chamber. The sample mount was loaded into the storage chamber overnight and further pumped down (for 1 to 2 h) before the analysis (Zhang *et al.*, 2018). A Cs^+ primary beam of 4-5 nA and Φ~15 μm (10 kV impact energy) was used to sputter secondary ion from the samples. The size of the analytical area was 30 μm × 30 μm (15 μm spot size + 15 μm rastering). The pre-sputtering process lasted for 170 seconds with a raster area of 50 μm × 50 μm, which is larger than the analysis area to minimize the water background signal. The normal-incidence electron gun and the nuclear magnetic resonance (NMR) controller were used to ensure charge compensation throughout the measurement session and to stabilize the magnetic field, respectively. Other instrument parameters include 2000 μm field aperture, 400 μm contrast aperture, 60 μm entrance slit, 80 μm max area, 173 μm exit slit, and 50 eV energy slit with 5 eV gap. The Faraday Cup detectors, located on L'2 trolley with 10^{10} Ohm amplifiers, and an electron multiplier of mono-collector were used to measure the $^{16}O^-$ and $^{16}O^1H^-$, respectively. For $^{16}O^-$, 500 mm collector slits were used to yield a ~2500 mass resolution power (MRP) with sufficiently flat plateau, while a ~173 μm collector slit was used for electron multiplier (yielding ~7000 MRP) to obtain a sufficiently flat plateau and separate isobaric interference of $^{17}O^-$ on $^{16}O^1H^-$. Background H_2O content was determined on standard San Carlos olivine as it has the lowest H_2O abundance among all standards. Water content was calculated according to the calibration curves established by analyses of the olivine standards of San Carlos (Fo = 91.1), KLB-1 (Fo = 89.3), ICH-30 (Fo = 90.6), and Mongok (Fo = 99.0) (Zhang *et al.*, 2020). The uncertainty of the calibrated water content is ~10 %. All data measured on standards and samples are listed in Table S-3 and S-4, respectively. The plot with H_2O calibration on the standards is shown in Table S-3.

Supplementary Tables

Table S-1 Water contents (μg.g-1) and major oxide compositions (wt. %) of olivine from Bursa and Lycian ophiolites in Türkiye.
Table S-2 Results of standards and working conditions of EPMA analysis.
Table S-3 Results of standards and the plot of water calibration on the standards of the SIMS analysis.
Table S-4 All SIMS data of samples.

Tables S-1 to S-4 are available for download (.xlsx) from the online version of this article at http://doi.org/10.7185/geochemlet.2530

Supplementary Figures

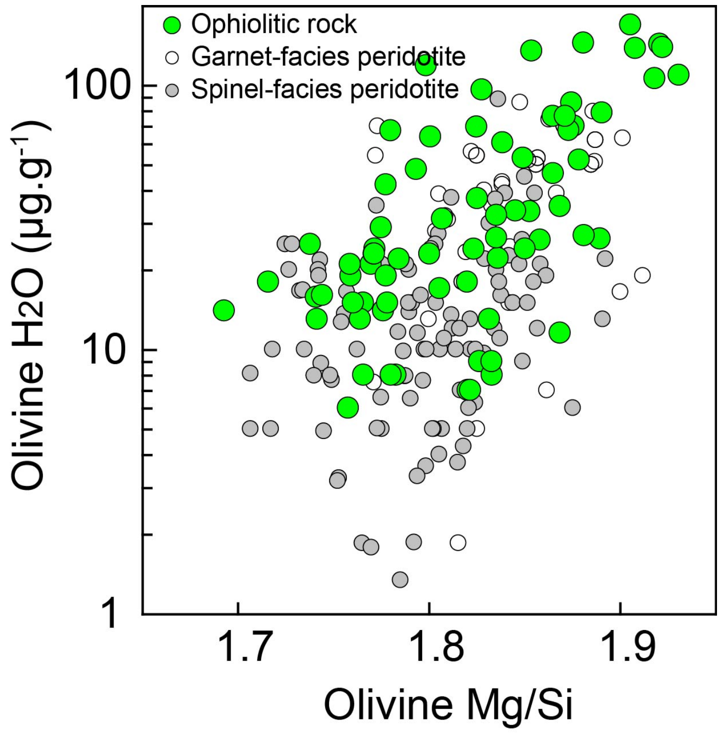

Figure S-1 Plot of H_2O ($\mu g.g^{-1}$) *vs.* Mg/Si for olivine from ophiolites, and mantle xenoliths. Data sources are as in Fig. 3.

Supplementary Information References

Cui, Z., Xia, X.P., Yang, Q., Zhang, K., Yang, X., Lai, C.K., Zhang, W.F., Zhang, Y.Q., Yang, Y.N. (2024) Ultralow H_2O content analysis with a large-geometry secondary ion mass spectrometer. *Journal of Analytical Atomic Spectrometry* 39, 1070-1076. https://doi.org/10.1039/d3ja00422h

Zhang, W.F., Xia, X.P., Zhang, Y.Q., Peng, T.P., Yang, Q. (2018) A novel sample preparation method for ultra-high vacuum (UHV) secondary ion mass spectrometry (SIMS) analysis. *Journal of Analytical Atomic Spectrometry* 33, 1559-1563. https://doi.org/10.1039/c8ja00087e

Zhang, W.F., Xia, X.P., Eiichi, T., Li, L., Yang, Q., Zhang, Y.Q., Yang, Y.N., Liu, M.L., Lai, C. (2020) Optimization of SIMS analytical parameters for water content measurement of olivine. *Surface and Interface Analysis* 52, 224-233. https://doi.org/10.1002/sia.6729

Additional References for Data Sources in Figures 2 and 3

Bai, Y., Cui, M.M., Su, B.X., Liu, X., Xiao, Y., Robinson, P.T., Gu, X.Y. (2024) FTIR study of H_2O in silicate minerals and mineral inclusions in chromite from the Peridotite Zone of the Stillwater Complex: evidence for chromitite formation in a H_2O-rich environment. *Geological Society of America Bulletin* 136, 1661-1674. https://doi.org/10.1130/B36733.1

Baptiste, V., Tommasi, A., Demouchy, S. (2012) Deformation and hydration of the lithospheric mantle beneath the Kaapvaal craton, South Africa. *Lithos* 149, 31-50. https://doi.org/10.1016/j.lithos.2012.05.001

Bell, D.R., Rossman, G.R., Maldener, J., Endisch, D., Rauch, F. (2003) Hydroxide in olivine: A quantitative determination of the absolute amount and calibration of the IR spectrum. *Journal of Geophysical Research: Solid Earth* 108, 2105. https://doi.org/10.1029/2001JB000679

Demouchy, S., Ishikawa, A., Tommasi, A., Alard, O., Keshav, S. (2015) Characterization of hydration in the mantle lithosphere: Peridotite xenoliths from the Ontong Java Plateau as an example. *Lithos* 212, 189-201. http://dx.doi.org/10.1016/j.lithos.2014.11.005

Demouchy, S., Jacobsen, S.D., Gaillard, F., Stern, C.R. (2006) Rapid magma ascent recorded by water diffusion profiles in mantle olivine. *Geology* 34, 429-432. https://doi.org/10.1130/G22386.1

Denis, C.M., Alard, O., Demouchy, S. (2015) Water content and hydrogen behaviour during metasomatism in the uppermost mantle beneath Ray Pic volcano (Massif Central, France). *Lithos* 236, 256-274. https://doi.org/10.1016/j.lithos.2015.08.013

Denis, C.M., Demouchy, S., Shaw, C.S. (2013) Evidence of dehydration in peridotites from Eifel Volcanic Field and estimates of the rate of magma ascent. *Journal of Volcanology and Geothermal Research* 258, 85-99. https://doi.org/10.1016/j.jvolgeores.2013.04.010

Doucet, L.S., Peslier, A.H., Ionov, D.A., Brandon, A.D., Golovin, A.V., Goncharov, A.G., Ashchepkov, I.V. (2014) High water contents in the Siberian cratonic mantle linked to metasomatism: an FTIR study of Udachnaya peridotite xenoliths. *Geochimica et Cosmochimica Acta* 137, 159-187. https://doi.org/10.1016/j.gca.2014.04.011

Grant, K., Ingrin, J., Lorand, J.P., Dumas, P. (2007) Water partitioning between mantle minerals from peridotite xenoliths. *Contributions to Mineralogy and Petrology* 154, 15-34. https://doi.org/10.1007/s00410-006-0177-1

Kempf, E.D., Hermann, J. (2018) Hydrogen incorporation and retention in metamorphic olivine during subduction: Implications for the deep water cycle. *Geology* 46, 571-574. https://doi.org/10.1130/G40120.1

Kurosawa, M., Yurimoto, H., Sueno, S. (1997) Patterns in the hydrogen and trace element compositions of mantle olivines. *Physics and Chemistry of Minerals* 24, 385-395. https://doi.org/10.1007/s002690050052

Li, P., Scott, J.M., Liu, J., Xia, Q.K. (2018) Lateral H_2O variation in the Zealandia lithospheric mantle controls orogen width. *Earth and Planetary Science Letters* 502, 200-209. https://doi.org/10.1016/j.epsl.2018.09.004

Matsyuk, S.S., Langer, K. (2004) Hydroxyl in olivines from mantle xenoliths in kimberlites of the Siberian platform. *Contributions to Mineralogy and Petrology* 147, 413-437. https://doi.org/10.1007/s00410-003-0541-3

Peslier, A., Luhr, J. (2006) Hydrogen loss from olivines in mantle xenoliths from Simcoe (USA) and Mexico: mafic alkalic magma ascent rates and water budget of the sub-continental lithosphere. *Earth and Planetary Science Letters* 242, 302-319. https://doi.org/10.1016/j.epsl.2005.12.019

Peslier, A.H., Woodland, A.B., Wolff, J.A. (2008) Fast kimberlite ascent rates estimated from hydrogen diffusion profiles in xenolithic mantle olivines from southern Africa. *Geochimica et Cosmochimica Acta* 72, 2711-2722. https://doi.org/10.1016/j.gca.2008.03.019

Peslier, A.H., Woodland, A.B., Bell, D.R., Lazarov, M. (2010) Olivine water contents in the continental lithosphere and the longevity of cratons. *Nature* 467, 78-81. https://doi.org/10.1038/nature09317

Su, B.X., Robinson, P.T., Chen, C., Xiao, Y., Melcher, F., Bai, Y., Gu, X.Y., Uysal, I., Lenaz, D. (2020) The occurrence, origin and fate of water in podiform chromitites. *American Mineralogist* 105, 894-903. https://doi.org/10.2138/am-2020-7270

Tang, D., Qin, K., Evans, N.J., Fang, L. (2023) Silicate mineral inclusions in chromite from the Eastern Bushveld complex: Implications for the origin and evolution of hydrous melt during chromite mineralization in the Critical Zone. *Lithos* 438, 106997. https://doi.org/10.1016/j.lithos.2022.106997

Tang, D.M., Qin, K.Z., Su, B.X., Mao, Y.J., Evans, N.J., Fang, L.R. (2022) Addition of H_2O at the Baishiquan and Tianyu magmatic Ni-Cu sulfide deposits, southern Central Asian Orogenic Belt, China: evidence from isotopic geochemistry of olivine and zircon. *Mineralium Deposita* 57, 235-254. https://doi.org/10.1007/s00126-021-01063-2

Wang, Y.F., Ren, H.P., Jin, Z.M. (2016) Water and fabric in an ophiolitic peridotite from a supra-subduction zone. *Contributions to Mineralogy and Petrology* 171, 1-17. https://doi.org/10.1007/s00410-016-1234-z

Yang, X.Z., Xia, Q.K., Deloule, E., Dallai, L., Fan, Q.C., Feng, M. (2008) Water in minerals of the continental lithospheric mantle and overlying lower crust: a comparative study of peridotite and granulite xenoliths from the North China Craton. *Chemical Geology* 256, 33-45. https://doi.org/10.1016/j.chemgeo.2008.07.020

Yu, M., Wang, Q., Yang, J.S., (2019) Fabrics and water contents of peridotites in the Neotethyan Luobusa ophiolite, southern Tibet: implications for mantle recycling in supra-subduction zones. *Journal of the Geological Society* 176, 975-991. https://doi.org/10.1144/jgs2018-152

Zhang, W.F., Xia, X.P., Su, B.X., Xu, Y.G., Zhang, Y.Q., Yang, Q., Zhang, L., Cui, Z.X., (2022) Distinct geochemical behavior of water in olivine between silicate and carbonatite metasomatism. *Minerals* 12, 1090. https://doi.org/10.3390/min12091090

Zhu, B.B., Wang, Q., Wang, L.S., Chen, L.H., Zhang, H.F., 2009. Water content of peridotite xenoliths from Cenozoic basalt in Yangyuan, Hebei province. *Geological Journal of China Universities* 15, 263-272 (in Chinese with English abstract).